Supermirror Polarizer for the FnPB Cold Line

Chris Crawford

2007-10-04

A ballistic neutron transport simulation has been performed to optimize construction of a supermirror bender polarizer for the cold neutron guide of the SNS FnPB. The simulation was based the McStas[1] model of the FnPB developed by Paul Huffman[2], used previously to optimize the chopper opening angles for the NPDGamma experiment [3].

1 Design Considerations

Recent improvements in the m-value, polarization output, and size of magnetized supermirrors, as well as potential issues in the performance of ^{3}He spin filter at high luminosity have prompted reconsideration of a supermirror bender polarizer (SMpol) for the FnPB cold line. The SMpol has two advantages: higher polarization and larger cross section area, each of which contributes a factor of two to increasing the figure of merit.

For maximum transmission, the polarizer should have the same cross section as the rest of the guide, 10×12 cm^2. The polarizer section is curved to block the line-of-sight of neutrons which would pass through without reflecting off any magnetized surface. The bend should be very gradual to preserve the phase space of the neutrons passing through and not decrease the transmission. Therefore, the bender is segmented with $n \approx 50$ polarized supermirror lamellas in the direction of the bend to reduce the bend angle in each channel. If the channel width d is excessively narrow, the neutrons will suffer extra reflections, reducing the transmission. Thus a balance must be achieved between polarization and transmission. The guide may be made shorter by increasing the number of channels; however, each channel also absorbs the neutrons incident on the end of each lamella between the channels. The ratio of lamella to total cross sectional area is called the geometry factor. The glass should contain boron to absorb the transmitted spin state of neutrons, producing soft 0.5 MeV gamma rays which are easily shielded.

The final consideration is the optimal length of the bender. A longer bender can have wider channels, decreasing the geometry factor. However if the length is longer a single piece of glass, then each piece must be aligned very precisely. Any mismatch will cause extra absorption. Typical maximum lengths are 400–420 mm for $d = 0.3$ mm borated glass from DESAG. The minimum thickness of float glass is 0.55 mm and of borofloat it is 0.7 mm, which is too thick [4].

An order of magnitude estimate of the optimal bend radius of curvature r for a bender of length l and channel width d is obtained by requiring every neutron to bounce at least once in the guide, or to block the line of sight through the channel, as in Fig. 1,

$$d \;=\; r(1-\cos\theta) \;\approx\; \tfrac{1}{2}\theta^2 \;\approx\; \frac{l^2}{8r}. \tag{1}$$

The width of an individual channel is governed by phase space considerations. The radius of curvature must be gentle enough not to lose neutrons reflecting steeper than the critical angle around the bend. The Maier-Leibnitz relation between incoming angle γ, concave reflection angle γ_a, the distance x of the neutron from the outer surface at the entrance, and the guide radius of curvature r is [5]

$$\gamma^2 = \gamma_a^2 - \frac{2x}{r}. \tag{2}$$

Using the relation $\gamma = q\lambda/4\pi$, the characteristic neutron wavelength (the minimum wavelength for a zigzag trajectory through the bender, instead of just Garland reflections along the concave surface) is

$$\lambda^* = \frac{4\pi}{q_c m}\gamma^*, \qquad \text{where} \quad \gamma^{*\,2} \equiv \frac{2d}{r} \tag{3}$$

is the characteristic angle, the reflection angle at the concave mirror of a neutron that just grazes the inner mirror. The acceptance phase space for three critical angles corresponding to different wavelengths is shown in Fig. 2. Combining Eqs. 1 and 3,

$$\frac{l}{2r} \;=\; \sqrt{\frac{2d}{r}} \;=\; \gamma^* \;=\; \frac{\lambda^* q_c m}{4\pi} \;\approx\; \frac{1}{96}, \tag{4}$$

where $\lambda^* \approx 2$ for the wavelength range of interest 2.3 Å $< \lambda <$ 6 Å, $q_c = 0.0217$ Å^{-1} for ^{58}Ni, and for an $m = 3$ supermirror coating on the convex surface. For example, a 40 cm long bender would have a radius of curvature $r \approx 19$ m and channel width $d \approx 1.0$ mm, corresponding to 100 channels. Realistically it is better to straighten out the guide or increase the channel width to reduce the number of reflections.

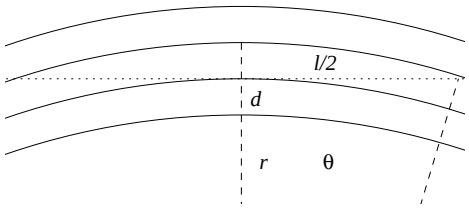

Figure 1: Three-channel bender at threshold of blocking the line of sight of neutrons.

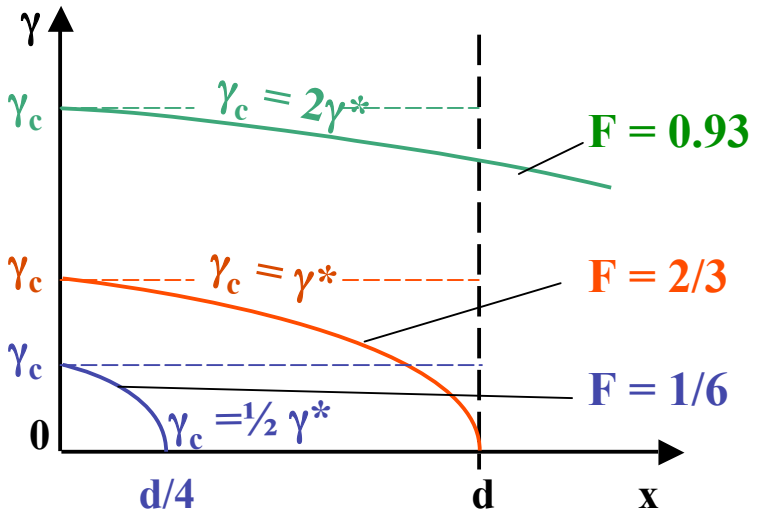

Figure 2: Phase space accepted by the bender, in terms of position $0 < x < d$ along the channel entrance and neutron angle $|\gamma| < \gamma_c$, for different wavelengths λ_c with critical reflection angle $\gamma_c = \lambda_c q_c m/4\pi$. The bender is filled ($F$) efficiently for $\gamma_c^2 \gg \gamma^{*2} = \frac{2d}{r}$, for channel width d and bend radius r [5].

2 McStas Simulation Code

The McStas simulation if the FnPB cold guide used the instrument definition file `Polychromatic_pre.instr`, based on `Polychromatic.instr`, used for the chopper simulations[3]. This simulation was run once, creating an ntuple listing the state of each neutron at the end of the guide, as well as the information described in Ref. [3]. The ntuple was booked with the component `Ntuple.comp`, also described in Ref. [3].

This ntuple was used as input for repeated simulations of the supermirror polarizer, using the instrument definition `Polychromatic_sm.instr`. A new component `Nsource.comp` was written to read the ntuple file as a neutron source. The McStas standard component `Virtual_input.comp` was not used because of a bug which affected reading long input lists. It component would cycle through the first block of events instead of reading the whole file, resulting in redundant statistics.

The SMpol was implemented in `SM_Bender.comp`, modified from the standard component `Bender.comp` to handle polarization states. Polarization information was included in the output ntuple by adding separate R_+ and R_- (or alternatively P curves). The output transmission was also modified as the average of the two neutron spin states. The code was also modified to accept more general reflectivity definitions. The different reflectivity profiles were plotted using the same code in `refl_profile.C` to verify their shape (Fig. 3). The

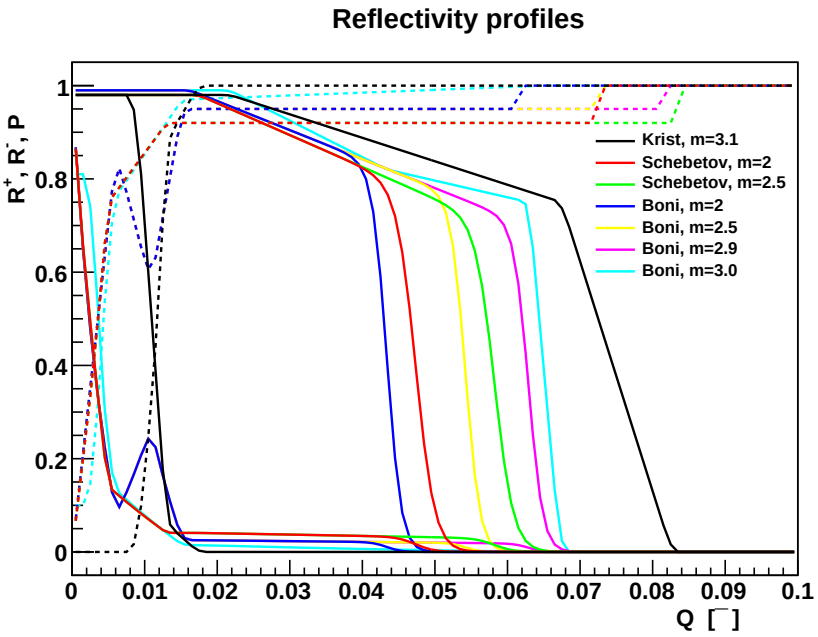

Figure 3: All reflectivity profiles used to simulate the SMpol.

code calculates the exact neutron trajectory analytically using cylindrical geometry, as opposed to propagating the neutron through each mirror reflection. A careful check was done of all equations in the original code.

The NPDGamma figure of merit was calculated using the code `p2n_line.C` used in [3]. It simulated the two choppers (generalizable to all four), the RF Spin Flipper polarization, collimators, and attenuation in the LH_2 target. A switch was added to choose between simulating the transmission and polarization from the ^{3}He polarizer cell or from the SMpol.

The analysis code `sm_fom_opt.C` was written to analyze the ntuple and optimize SMpol for the NPDGamma experiment. Simulations were repeated varying the SMpol length l, radius of curvature r, and number of channels n. The affect of the thickness of the lamella, d, and various reflectivity profiles was also investigated. For each simulation, a single optimization of the SNS window phase was performed to calculate the FOM.

The software is available online on the NPDGamma SVN server, located at `sns.phys.utk.edu/svn/npdg/trunk/simulations/sns/choppers/mcstas` (r650).

3 Results

The simulation and optimization of the SMpol was done in two rounds before converging on a preferred solution. Since not all work was repeated in the second round the results of both are displayed, keeping in mind that some parameters of the preliminary simulations have changed.

3.1 Preliminary Simulations

The first optimization focused on a comparison of the performance due to the reflectivity profiles from different manufacturers. The three-dimension optimization was performed for each profile by simulating the figure of merit on a grid of parameters (l, n, r). R was optimized first followed by N to yield the functions $FOM_m, r_m, n_m(l)$. All simulations assumed glass thickness $d = 0.4$ mm. The numbers quoted for the cost are not realistic, but are proportional to nd, or the coating surface area.

Fig. 4 shows the individual optimization of r for each value of n and l for a single reflectivity profile. Fig. 5 shows the optimization of n for different lengths, for each reflectivity profile. In the limit as $nl \to 0$, the FOM as a function of surface area nl is the same for all lengths, but as n increases, longer reflectivity profiles take advantage of reduce geometry factors. Results from all six reflectivity profiles considered as a function of nl are summarized in Fig. 6. Finally, the neutron flux and gamma capture rate of the NPDGamma experiment is compared between the ^3He polarizer ($NL = 4$ Amg $\cdot$ cm, $P_3 = 0.60$) and SMpol (Krist profile) in Fig. 7. Numerical results are recorded in Table 8.

3.2 Final Simulations

Based on the preliminary results, and above design considerations, it was decided to use a SMpol of length $l = 40$ cm and channel width $d = 0.3$ mm. In the meantime, a new reflectivity profile, Böni $m = 3.0$ was learned of. The reflectivity data and approximation for this coating are shown in Fig. 9. Note that this data was for an improved $m = 2.9$ coating. The simulations were repeated to verify the old results and investigate incremental changes in switching to the new parameters from $(l, d, m) = (50\text{ cm}, 0.4\text{ mm}, 2.9)$ to $(42\text{ cm}, 0.3\text{ mm}, 3.0)$. The changes in the FOM were $(-2.8\%, 4.8\%, 12.8\%)$ for respective changes in (l, d, m), resulting in an overal gain in the figure of merit. The main contributor was the improved shape of the Böni R_- profile at low q for $m = 3.0$. This profile no longer has a dip in the polarization at low q. The length $l = 40$cm was chosen to be comfortably within manufacturing specs, and had little affect on the FOM.

The m value of the inner (convex) surface coating was also investigated. It was found the the FOM was practically unchanged for $m = 2.5$ and $m = 2.0$. Therefore $m = 2.0$ was selected for the inner coating.

Additional investigations were done on the affect of collimation on the optimal bend radius r. While the FOM decreased by 3.3% and 38% from the addition of 15 cm and 10 cm collimators, respectively, placed 85 cm downstream of the bender, the optimal value n and r were very stable, as shown in Fig. 10. Note that the decrease in flux due to the 10 cm collimator is almost entirely due to the reduction in beam area: $1 - \pi(10\text{ cm}/2)^2/(10\text{ cm} \cdot 12\text{ cm}) = 34.5\%$. The extra 3.5% is due to divergence in the beam. The divergence is actually reduced by the SMpol, due to extra reflections at $m = 3$, not $m = 3.6$ like the rest of the guide. Fig. 11 shows the angular divergence in the beam before and after the bender.

Finally, the effect of lamella thickness was reinvestigated for d=0.3, 0.33, and 0.35 mm, were negligible, both in the FOM and optimal radius r.

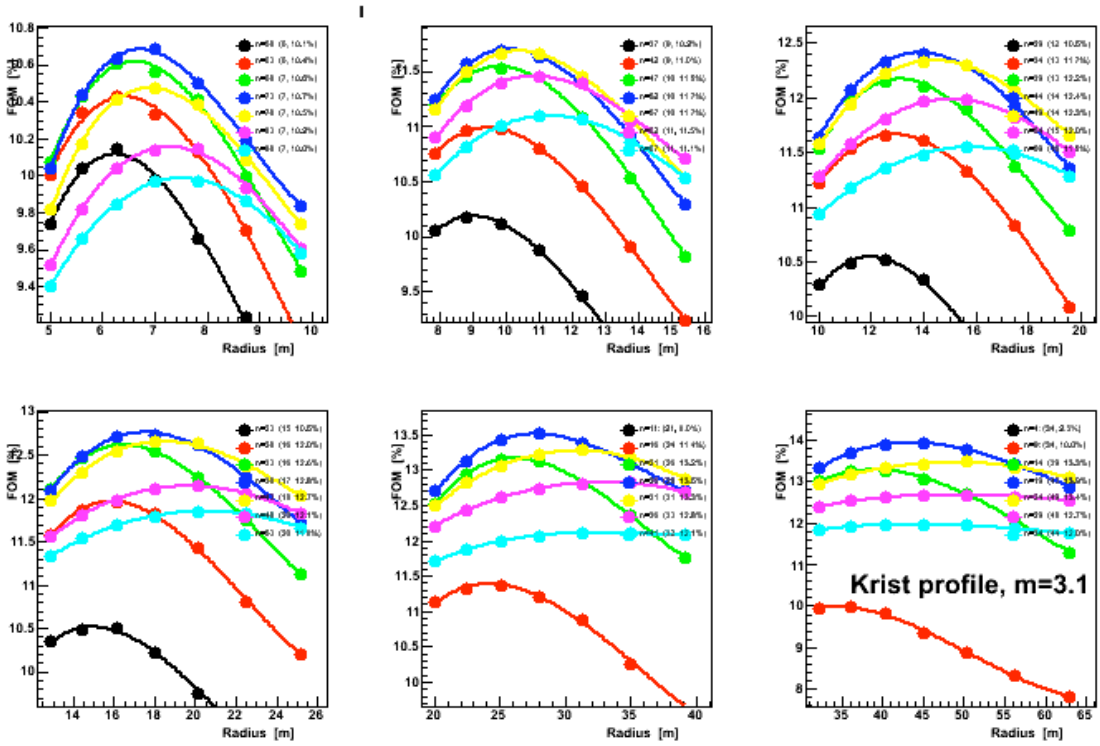

Figure 4: Optimization of the Krist $m = 3.1$ profile as a function of r for several values of n (separate colored lines). Each plot is for a separate value of $l = 0.2$, 0.3, 0.4, 0.5, 0.8, and 1.2 m.

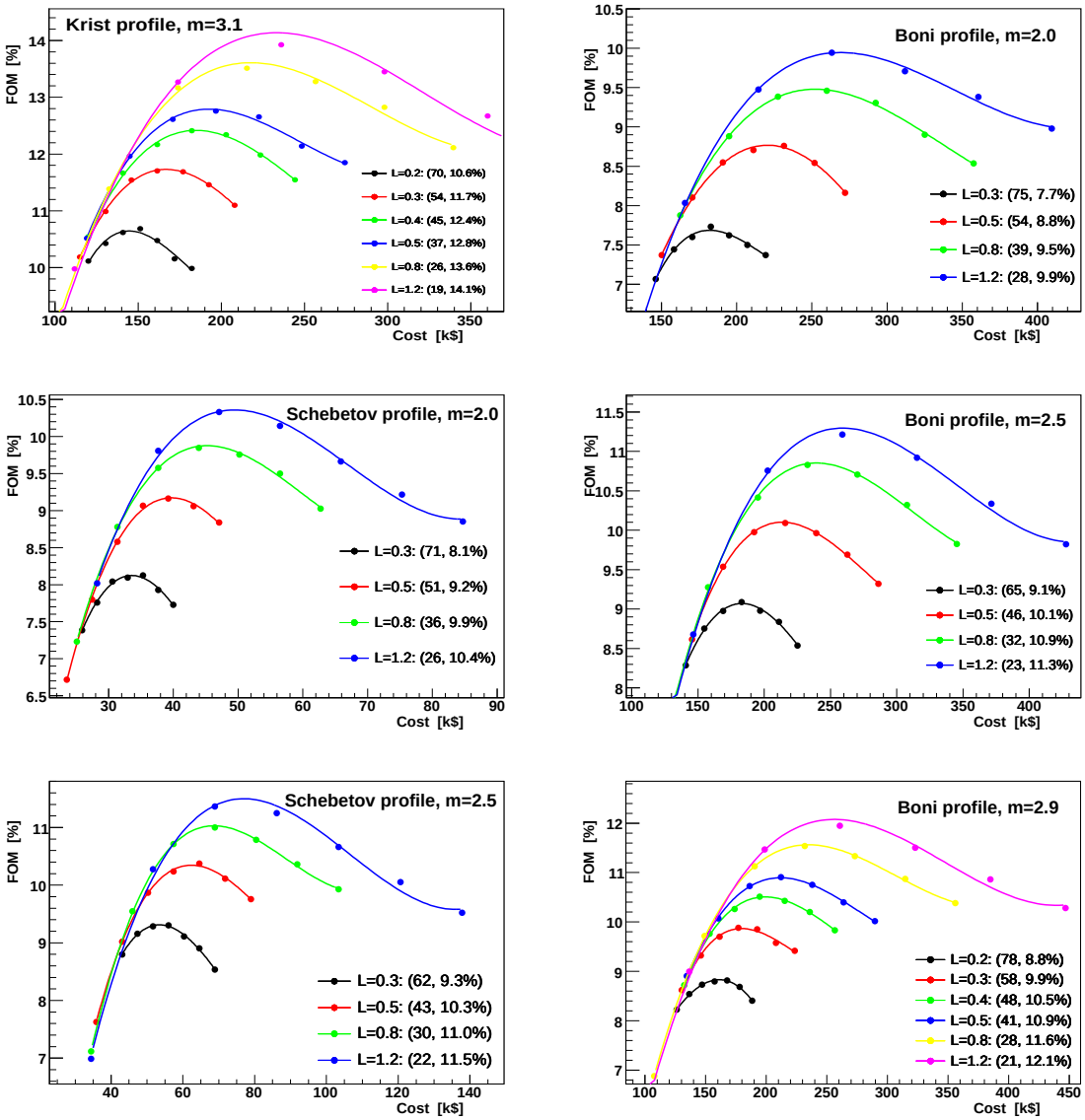

Figure 5: Optimization of each reflectivity profile as a function of n for several values of l. The cost is proportional to nl.

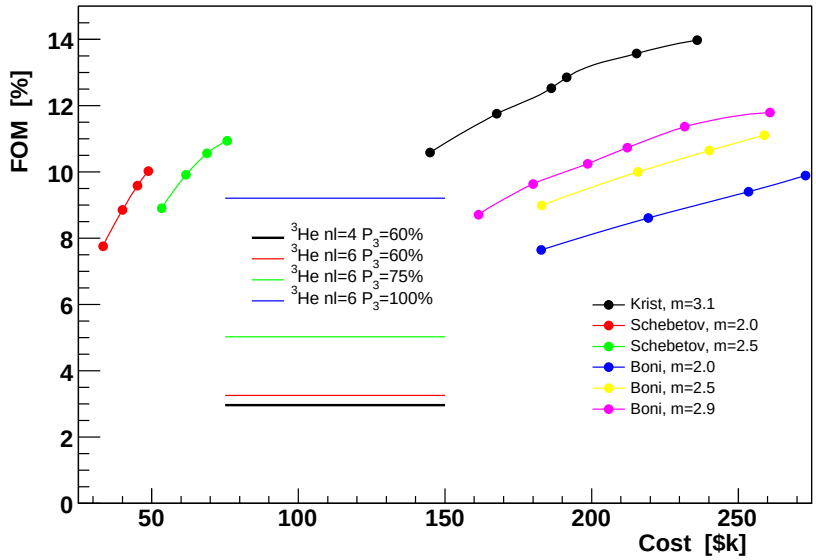

Figure 6: Summary of the results from Fig. 5 plotted versus nl. The figure of merit of a ^{3}He cell is shown for comparison.

4 Conclusions

It was decided to $n = 45$ channels instead of the optimal $n = 52$ because of only a 7% drop in the FOM at a cost savings of \$20k. The complete set design parameters chosen are: $l = 40$ cm, $n = 45$, $r = 14.8$ m, and $d = 0.3$ mm. For these values of (l, n, r, d) the characteristic wavelength is $\lambda^* = 1.23$ Å, a little more conservative than the initial estimate. A little tighter bend radius $r = 12.3$ would be needed to block line-of-sight, but the results of the optimization are consistent with the preliminary considerations. The Böni $m = 3.0$ reflection profile was chosen for the concave surface, and had a sizable improvement over the previous $m = 2.9$ profile. The standard $m = 2.0$ coating was selected for the inner surface, and had no effect on the FOM. The technical specifications for the outer coatings are shown in Fig. 12. The resulting FOM is expected to be 11.8%, compared with the FOM of 2.96% of an optimized ^{3}He cell with ^{3}He polarization $P_3 = 60\%$. Note this FOM includes chopper, collimation, depolarization, and capture in the LH_2 target, not just the performance of the SMpol. The transmission and polarization of the SMpol are 30.3% and 96.2%, respectively, in the simulation. This represents a factor of 4.0 improvement over the ^{3}He cell at Los Alamos.

References

[1] K. Lefmann and K. Nielsen, "McStas, a General Software Package for Neutron Ray-tracing Simulations", Neutron News **10**, 20 (1999); `http://mcstas.org`.

[2] P. R. Huffman, *et al.*, J. Res. Natl. Inst. Stand. Technol. **110**, 161 (2005); P. R. Huffman, *et al.*, *Beamline Performance Simulations for the Fundamental Neutron Physics Beamline*, 2005 (unpublished).

[3] C. B. Crawford, R. Mahurin, unpublished technical note, "Opening angles for the SNS FnPB choppers", 2006-11-30.

[4] P. Böni, private communication, 2007-08-21.

[5] R. Gähler, "Neutron Optics and Polarization", talk presented at the First Summer School on Fundamental Neutron Physics, Knoxville, 2006-06-05; `http://neutron.physics.ncsu.edu/SummerSchool/Gahler.ppt`

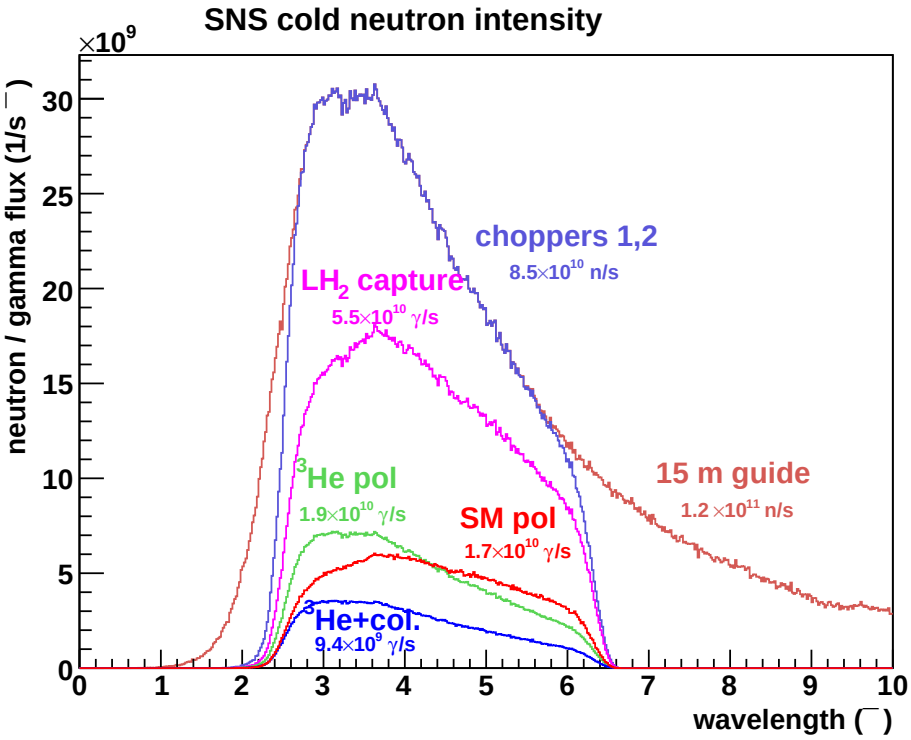

Figure 7: Neutron flux with and without the two choppers; gamma capture rate, with and without the SMpol or ^{3}He cell plus 9.0 cm collimator.

3He polarizer

merit	nl	p3[%]	FOM[%]=	(p2n /	beam) =	chop *	col *	TX *	cap *	(POL *	depol)^2;	Tx*Pol^2
0.71	4.0	50	2.09	0.2540	12.1373	70.37	48.82	34.76	59.75	55.30	97.94	10.63
(1.00)		60	2.96	0.3591	12.1373	70.37	48.82	37.38	60.05	63.30	97.86	14.98
1.52		75	4.51	0.5470	12.1373	70.37	48.82	42.46	60.55	73.14	97.67	22.71
2.63		100	7.79	0.9451	12.1373	70.37	48.82	54.66	61.55	84.59	97.04	39.11
0.78	6.0	50	2.31	0.2803	12.1373	70.37	48.82	23.17	59.12	71.47	98.02	11.84
1.10		60	3.26	0.3960	12.1373	70.37	48.82	26.55	59.60	79.11	97.94	16.62
1.70		75	5.03	0.6110	12.1373	70.37	48.82	33.41	60.36	87.19	97.76	25.40
3.11		100	9.21	1.1184	12.1373	70.37	48.82	51.60	61.78	94.58	96.99	46.16

Krist, m=3.1

merit	cost[$k]	l[m]	n[#]	r[m]	b[deg]	FOM[%]=	(p2n /	beam) =	chop *	col *	TX *	cap *	(POL *	depol)^2;	Tx*Pol^2
3.58	144.9	0.2	70	6.6	1.7	10.59	1.2851	12.1315	70.37	100.00	27.19	63.64	95.90	97.27	25.01
3.97	167.7	0.3	54	10.2	1.7	11.75	1.4257	12.1315	70.37	100.00	29.95	63.38	96.41	97.29	27.84
4.24	186.3	0.4	45	13.9	1.6	12.53	1.5203	12.1315	70.37	100.00	31.77	63.29	96.79	97.23	29.76
4.34	191.5	0.5	37	17.3	1.7	12.85	1.5588	12.1315	70.37	100.00	32.78	63.29	96.54	97.17	30.55
4.59	215.3	0.8	26	28.6	1.6	13.57	1.6461	12.1315	70.37	100.00	34.66	63.13	96.61	97.16	32.35
4.73	236.0	1.2	19	44.0	1.6	13.98	1.6962	12.1315	70.37	100.00	35.63	63.02	96.78	97.21	33.37

Schebetov, m=2.0

merit	cost[$k]	l[m]	n[#]	r[m]	b[deg]	FOM[%]=	(p2n /	beam) =	chop *	col *	TX *	cap *	(POL *	depol)^2;	Tx*Pol^2
2.62	33.4	0.3	71	14.1	1.2	7.76	0.9409	12.1315	70.37	100.00	20.99	63.85	93.48	97.01	18.34
2.99	40.0	0.5	51	23.8	1.2	8.85	1.0734	12.1315	70.37	100.00	23.49	63.63	94.53	97.03	20.99
3.24	45.2	0.8	36	39.1	1.2	9.59	1.1638	12.1315	70.37	100.00	25.35	63.37	94.77	97.20	22.77
3.39	48.9	1.2	26	59.0	1.2	10.03	1.2162	12.1315	70.37	100.00	26.45	63.26	95.09	97.03	23.92

Schebetov, m=2.5

merit	cost[$k]	l[m]	n[#]	r[m]	b[deg]	FOM[%]=	(p2n /	beam) =	chop *	col *	TX *	cap *	(POL *	depol)^2;	Tx*Pol^2
3.01	53.4	0.3	62	11.9	1.4	8.90	1.0800	12.1315	70.37	100.00	23.96	63.69	93.76	97.11	21.06
3.35	61.7	0.5	43	20.1	1.4	9.91	1.2019	12.1315	70.37	100.00	26.49	63.49	94.25	97.07	23.53
3.57	68.9	0.8	30	33.2	1.4	10.56	1.2816	12.1315	70.37	100.00	28.23	63.28	94.42	97.09	25.17
3.70	75.8	1.2	22	50.4	1.4	10.94	1.3276	12.1315	70.37	100.00	29.01	63.10	95.00	97.03	26.18

Boni, m=2.0

merit	cost[$k]	l[m]	n[#]	r[m]	b[deg]	FOM[%]=	(p2n /	beam) =	chop *	col *	TX *	cap *	(POL *	depol)^2;	Tx*Pol^2
2.59	182.8	0.3	75	15.0	1.1	7.65	0.9282	12.1315	70.37	100.00	19.86	64.03	95.01	97.33	17.93
2.91	219.4	0.5	54	25.3	1.1	8.61	1.0444	12.1315	70.37	100.00	22.14	63.77	95.80	97.17	20.32
3.18	253.5	0.8	39	41.5	1.1	9.40	1.1407	12.1315	70.37	100.00	24.00	63.49	96.46	97.09	22.33
3.34	273.0	1.2	28	61.3	1.1	9.89	1.2001	12.1315	70.37	100.00	25.00	63.47	96.81	97.23	23.43

Boni, m=2.5

merit	cost[$k]	l[m]	n[#]	r[m]	b[deg]	FOM[%]=	(p2n /	beam) =	chop *	col *	TX *	cap *	(POL *	depol)^2;	Tx*Pol^2
3.04	182.9	0.3	65	12.5	1.4	8.99	1.0901	12.1315	70.37	100.00	23.23	63.74	95.40	97.34	21.14
3.38	215.8	0.5	46	21.4	1.3	10.00	1.2130	12.1315	70.37	100.00	25.80	63.47	95.79	97.25	23.67
3.60	240.2	0.8	32	34.9	1.3	10.65	1.2915	12.1315	70.37	100.00	27.46	63.30	96.04	97.15	25.33
3.76	258.9	1.2	23	51.9	1.3	11.11	1.3478	12.1315	70.37	100.00	28.36	63.23	96.56	97.18	26.44

Boni, m=2.9

merit	cost[$k]	l[m]	n[#]	r[m]	b[deg]	FOM[%]=	(p2n /	beam) =	chop *	col *	TX *	cap *	(POL *	depol)^2;	Tx*Pol^2
2.94	161.4	0.2	78	7.5	1.5	8.71	1.0567	12.1315	70.37	100.00	22.93	63.58	94.75	97.24	20.59
3.26	180.1	0.3	58	11.2	1.5	9.64	1.1699	12.1315	70.37	100.00	25.41	63.57	94.84	97.13	22.86
3.46	198.7	0.4	48	15.1	1.5	10.25	1.2434	12.1315	70.37	100.00	26.65	63.45	95.42	97.26	24.26
3.63	212.2	0.5	41	18.9	1.5	10.73	1.3012	12.1315	70.37	100.00	27.74	63.39	95.82	97.17	25.47
3.84	231.8	0.8	28	31.2	1.5	11.36	1.3778	12.1315	70.37	100.00	29.48	63.23	95.76	97.16	27.03
3.98	260.8	1.2	21	47.1	1.5	11.79	1.4299	12.1315	70.37	100.00	30.27	63.03	96.59	97.00	28.24

Boni, m=3.0 --- Final Simulation ---

merit	cost[$k]	l[m]	n[#]	r[m]	b[deg]	FOM[%]=	(p2n /	beam) =	chop *	col *	TX *	cap *	(POL *	depol)^2;	Tx*Pol^2
3.78	165.6	0.4	40	14.3	1.60	11.19	1.3569	12.1315	70.37	100.00	29.86	64.39	93.69	97.05	28.12
4.01	186.3	0.4	45	14.8	1.55	11.85	1.4380	12.1315	70.37	100.00	30.31	63.84	96.15	97.03	28.54
4.07	207.0	0.4	50	15.4	1.49	12.05	1.4621	12.1315	70.37	100.00	30.32	63.38	97.22	97.11	28.59

Figure 8: Numerical results for optimized r. `merit` is the FOM normalized to the LANSCE ^{3}He cell at $P_3 = 0.60$. `FOM` equals the gamma rate $\times$ the P^2 in the target (`p2n`), normalized to the unchopped neutron rate (`beam`) [10^{10} s^{-1}]. Transmissions: choppers (`chop`), 9 cm collimator (`col`), polarizer (`TX`), and probability of neutron capture (`cap`). `depol` is depolarization in the spin flipper. The last column is the FOM of the polarizer only.

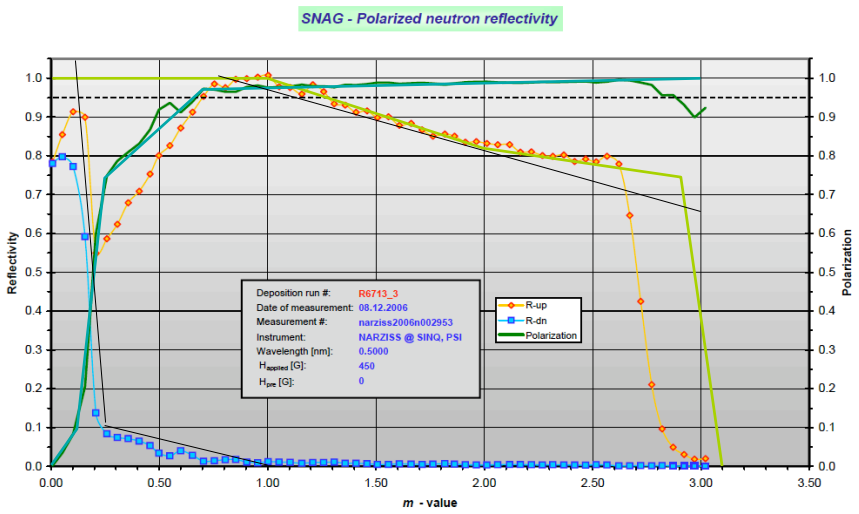

Figure 9: New reflectivity data for an $m = 2.9$ remanent supermirror from Peter Böni [4]. The straight lines are the approximation used in the simulations for an $m = 3.0$ supermirror.

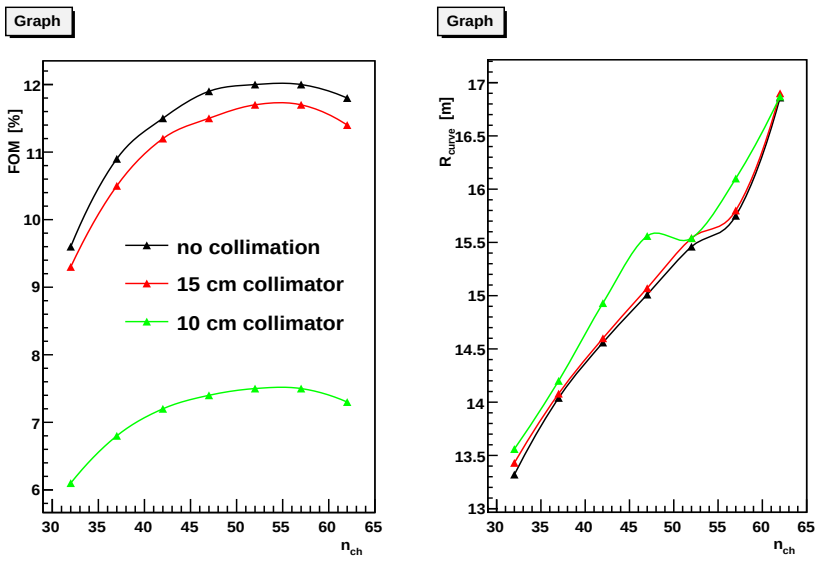

Figure 10: The figure of merit and optimal radius of curvature

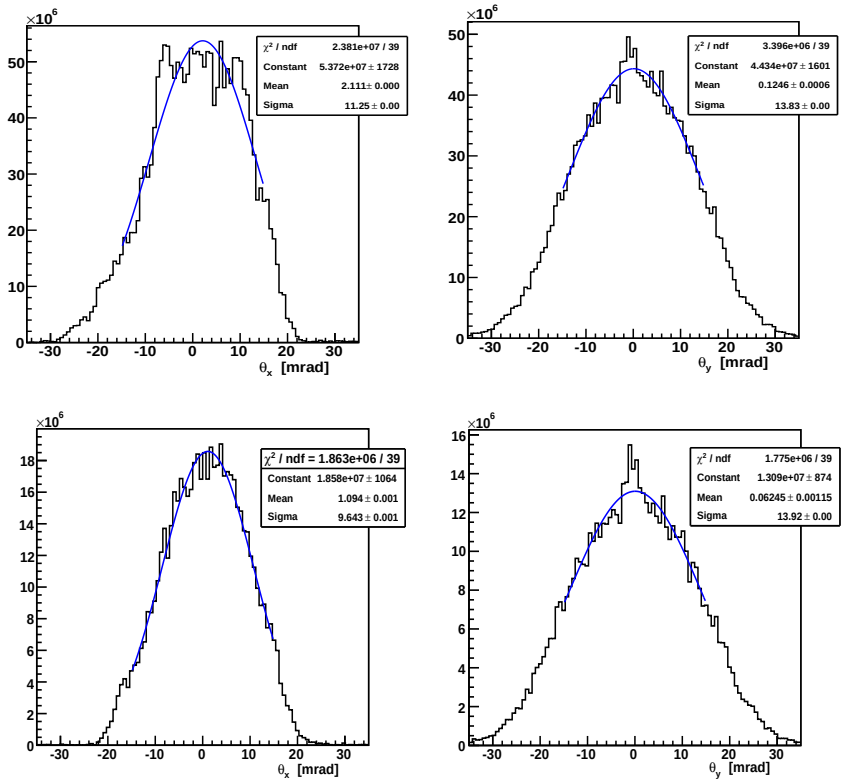

Figure 11: Angular profile in horizontal (left) and vertical (right) direction of beam before (top) and after (bottom) the SMpol.

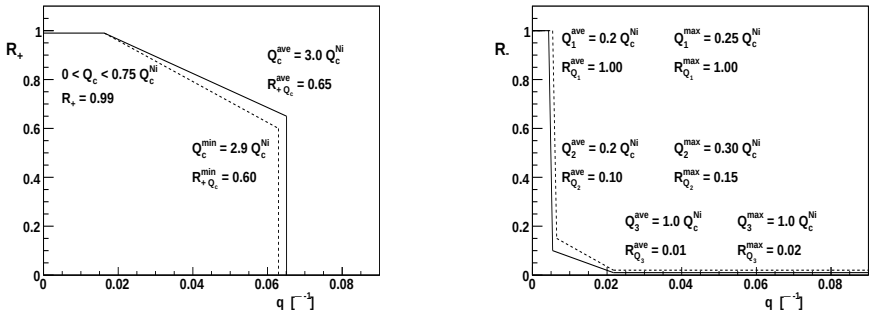

Figure 12: Minimum specifications for supermirror coatings in construction of polarizer bender.